Data fusion of SPOT and LANDSAT images using additive multiresolution wavelet decomposition

Jorge Núñez[a,b], Xavier Otazu[a,b], Octavi Fors[a,b], Albert Prades[c], Vicenç Palà[d] and Román Arbiol[d]

[a]Departament d'Astronomia i Meteorologia, Universitat de Barcelona, E-08028 Barcelona, Spain.

[b] Observatori Fabra, Barcelona, Spain.

[c]Escola Universitaria Politècnica de Barcelona, U.P.C., E-08028 Barcelona, Spain.

[d] Institut Cartogràfic de Catalunya, Parc de Montjuïc, E-08038 Barcelona, Spain.

ABSTRACT

In this paper we present the development of a technique, based on multiresolution wavelet decomposition, for the merging and data fusion of a high-resolution panchromatic image and a low-resolution multispectral image. The method presented here consists of adding the wavelet coefficients of the high-resolution image to the multispectral (low-resolution) data. We have studied several possibilities concluding that the method which produces the best results consists in adding the high order coefficients of the wavelet transform of the panchromatic image to the intensity component (defined as $L = \frac{R+G+B}{3}$) of the multispectral image. Using this method, the detail information from both images is preserved. The method is capable of enhancing the spatial quality of the multispectral image while preserving its spectral content to a grater extent. The method presented does not modify the total energy of the multispectral image, since the mean value of each of the added wavelet planes is 0. The method is, thus, an improvement on standard Intensity-Hue-Saturation (IHS or LHS) mergers. We used the method to merge SPOT and LANDSAT (TM) images. The technique presented is clearly better than the IHS and LHS mergers in preserving both spectral and spatial information.

Keywords: Data fusion, Image merging, Wavelet decomposition, Multiresolution,

1. INTRODUCTION

There are several situations that simultaneously require high spatial and high spectral resolution in a single image. This is particularly important in remote sensing. In other cases, for example astronomy, high spatial resolution and high signal-to-noise ratio may be required . However, in most cases instruments are not capable of providing such data either by design or because of observational constraints. For example, in remote sensing, SPOT PAN satellite provides high-resolution (10-m pixels) panchromatic data, while LANDSAT TM satellite data provides lower-resolution (30-m pixels) multispectral images. In astronomy, the space-borne telescopes give high-resolution images but the photons are expensive to collect, making long-exposure multispectral observations unusual. From the ground, on the other hand, the resolution is poor but the photons are cheap to collect and the signal-to-noise ratio can be increased. Besides it is easy to obtain long-exposure (but low-resolution) multispectral data from the ground.

One possible solution comes from the field of data fusion.[1] A number of methods have been proposed for merging panchromatic and multispectral data.[2,3] The most common procedures are the Intensity-Hue-Saturation transform based methods (IHS and LHS mergers).[4,5] However, the IHS and LHS methods produce spectral degradation. This is particularly crucial in remote sensing if the images to merge were not taken at the same time. In the last few years multiresolution analysis has become one of the most promising methods for the analysis of images in remote sensing.[6] Recently, several authors (Yocky,[7,8] Garguet-Duport et al.,[9] Ranchin et al.[10]) proposed a new approach to image merging that uses a multiresolution analysis procedure based upon the discrete two-dimensional wavelet transform.

Other author information: (Send correspondence to J.N.)
J.N.: E-mail: jorge@fajnm1.am.ub.es
X.O.: E-mail: xavier@fajnm1.am.ub.es
O.F.: E-mail: octavi@fajnm1.am.ub.es
A.P.: E-mail: albert@mercator.upc.es
V.P.: E-mail: vicencp@icc.es
R.A.: E-mail: arbiol@icc.es

We[11] also carried out a preliminary study of the wavelet-based method in combination with image reconstruction. The wavelet approach preserves the spectral characteristics of the multispectral image better than the standard IHS or LHS methods.

Wavelet-based image merging can be performed in two ways: a) by replacing some wavelet coefficients of the multispectral image by the corresponding coefficients of the high-resolution image and b) by adding high-resolution coefficients to the multispectral data. Here, we further explore the wavelet transform image merging technique with special attention to the "additive" merger. To decompose the data into wavelet coefficients, we use the discrete wavelet transform algorithm known as "à trous" ("with holes"). The method is applied to merge SPOT and LANDSAT (TM) images.

2. STANDARD MERGING METHODS

The standard merging methods are based on the transformation of the RGB multispectral channels into the Intensity-Hue-Saturation components.[12] Intensity refers to the total color brightness, Hue refers to the dominant or average wavelength contributing to a color and Saturation refers to the purity of a color relative to gray. In the standard methods the usual steps to perform are the following:

1) Register the low-resolution multispectral image to the same size as the high-resolution panchromatic image in order to be superimposed.

2) Transform the R, G and B bands of the multispectral image into the Intensity-Hue-Saturation components.

3) Modify the high-resolution panchromatic image to take into account the spectral differences with respect to the multispectral image, the different atmospheric and illumination conditions, etc. This is usually performed by conventional histogram matching between the panchromatic image and the intensity component of the Intensity-Hue-Saturation representation. Specifically, after computing the histogram of both the panchromatic image and the Intensity component of the multispectral, the histogram of the Intensity (of the multispectral) is used as reference to which we match the histogram of the panchromatic image.

4) Replace the intensity component by the panchromatic image and perform the inverse transformation to obtain the merged RGB image with merged panchromatic information.

Throughout this paper we assume that all R,G,B values are scaled over the range 0,255.

The result of the standard merging methods depends on the Intensity-Hue-Saturation system used. Many Intensity-Hue-Saturation transformation algorithms have been developed for converting the RGB values. While the complexity of the models varies, they produce similar values for hue and saturation. However, the algorithms differ in the method used in calculating the intensity component of the transformation. The most common intensity definitions are:

$$I = I(R,G,B) = max(R,G,B)$$

$$L = L(R,G,B) = \frac{R+G+B}{3}$$

$$L' = L'(R,G,B) = \frac{max(R,G,B)+min(R,G,B)}{2}$$

We call the systems based on these definitions IHS, LHS and L'HS color systems respectively. The first system (based on I), also known as the Smith's hexcone,[12] ignores two of the components to compute the intensity and will produce equal intensity for a pure color eg: $I = I(255,0,0) = 255$ and for a white pixel $I = I(255,255,255) = 255$. However, the second system (based on L), known as Smith's triangle model,[12] would produce intensities of $L = L(255,255,255) = 255$ for a white pixel but only $L = L(255,,0,0) = 85$ for a pure color. The third system (based on L')[13] would again produce a result of $L' = L'(255,255,255) = 255$ for the white pixel, and $L' = L'(255,0,0) = 125$ for a pure color.

Furthermore, the transformation algorithm based on the third definition (L') shows bizarre behavior in some cases. For example, if we have RGB values of $(R,G,B) = (100,150,200)$, transform them to L'HS system obtaining $(L'HS) = (150,210,0.476)$, add 10 counts (over a maximum of 255) to the L' component (now $L' = 160$) and reverse the transformation ($R = R(160,210,0.476) = 115; G = G(160,210,0.476) = 160; B = B(160,210,0.476) = 205$), the resulting RGB values are $(R,G,B) = (115,160,205)$ i.e. the color with the lowest value (R) is the one which has largest increment, while the component with highest value (B) has the lowest increment. On the other hand, if we transform the same RGB values $(R,G,B) = (100,150,200)$, to the LHS system obtaining $(LHS) = (150,210,0.333)$

and again add 10 counts to the L component (now $L = 160$) and reverse the transformation, the RGB values would be $(R, G, B) = (107, 160, 213)$. In this case, the increment of 10 counts in the intensity is distributed proportionally to the values of the R, G and B components.

Thus, in this paper we prefer the definition $L = \frac{R+G+B}{3}$ for the intensity component although we will use both IHS and LHS based standard merging methods to compare our results. When this component is defined as $L = \frac{R+G+B}{3}$ it is also called Lightness.

3. WAVELET DECOMPOSITION

Multiresolution analysis based on the wavelet theory permits the introduction of the concepts of details between successive levels of scale or resolution.[14-19]

Wavelet decomposition is increasingly being used for the processing of images.[20,21] The method is based on the decomposition of the image into multiple channels based on their local frequency content. The wavelet transform provides a framework to decompose images into a number of new images, each one of them with a different degree of resolution. The wavelet representation is an intermediate representation between the Fourier and the spatial representation. In the Fourier Transform we know the global frequency content of our image, but we have no information about the spatial localization of these frequencies. However, the wavelet transform gives us an idea of both the local frequency content and the spatial distribution of these frequencies. Since in Fourier space the base functions are sinusoidal, they extends along all space and do not have spatial concentration. But wavelets are concentrated around a central point, thus they have a high degree of spatial localization.

3.1. Some Theory

We will shortly present the basics of the wavelet transform relying in the multiresolution signal representation concept.[6] We present here 1-dimensional formulas that can be easily extended to the 2-dimensional case.

Given a signal $\mathbf{f}(t)$, we construct a sequence $F_m(\mathbf{f}(t))$ of approximations of $\mathbf{f}(t)$. Each $F_m(\mathbf{f}(t))$ is specific for the representation of the signal at a given scale (resolution). $F_m(\mathbf{f}(t))$ represents the projection of the signal $\mathbf{f}(t)$ from the signal space $\mathbf{S}$ onto subspace $\mathbf{S_m}$. In this representation, $F_m(\mathbf{f}(t))$ is the "closest" approximation of $\mathbf{f}(t)$ with resolution 2^m.

The differences between two consecutive scales $m+1$ and m are the multiresolution wavelet planes or "detail" signal at resolution 2^m:

$$w_m(\mathbf{f}(t)) = F_{m+1}(\mathbf{f}(t)) - F_m(\mathbf{f}(t)). \tag{1}$$

This detail signal can be expressed as:

$$w_m(\mathbf{f}(t)) = \sum_n W_{m,n}(\mathbf{f})\psi_{m,n}(t) \tag{2}$$

where coefficients $W_{m,n}(\mathbf{f})$ are given by the *direct wavelet transform of the of the signal* $\mathbf{f}$(t):

$$W_{m,n}(\mathbf{f}) = \int_{-\infty}^{+\infty} \mathbf{f}(t)\,\psi_{m,n}(t)dt\ . \tag{3}$$

In the direct wavelet transform (3), m and n are scaling and translational parameters respectively. The coefficients $W_{m,n}(\mathbf{f})$ are called wavelet coefficients of $\mathbf{f}(t)$. Such coefficients correspond to the fluctuations of the signal $\mathbf{f}(t)$ near the point n at resolution level m. Thus, the wavelet transform (3) represents the expansion of signal $\mathbf{f}(t)$ in the set of basis functions $\psi_{m,n}(t)$. These basis functions are a scaled and translated versions of a general function $\psi(t)$ called *Mother Wavelet*. To construct the basis functions $\psi_{m,n}(t)$, the *Mother Wavelet* $\psi(t)$ is dilated and translated according to parameters m and n as follows:

$$\psi_{m,n}(t) = 2^{m/2}\psi(2^m t - n)\ . \tag{4}$$

Using (4) we obtain an orthonormal wavelet basis.[16] Parameter m stretches or compresses the *Mother Wavelet*, modifying this function to produce a narrow or broader new function. Therefore, all the basis functions $\psi_{m,n}(t)$ have the same profile, that is, the Mother Wavelet profile, but dilated and translated according to parameters m and n respectively.

The *inverse discrete wavelet transform* is given by the reconstruction formula:

$$\mathbf{f}(t) = \sum_m \sum_n W_{m.n}(\mathbf{f}) \psi_{m,n}(t) \tag{5}$$

In summary, the wavelet transform describes at each resolution step the difference signal between the previous and the current resolution representation. By iterating the process from the highest to the lowest available resolution level we obtain a pyramidal representation of the signal. The advantage of the wavelet transform defined above is that it relies in an orthogonal transform, so the information difference from one resolution level to the next one is non-redundant.

3.2. The "à trous" algorithm

To obtain a discrete wavelet decomposition for images, we follow Starck and Murtagh,[22] and we use the discrete wavelet transform algorithm known as "à trous" ("with holes") to decompose the image into wavelet planes. Given an image $\mathbf{p}$ we construct the sequence of approximations:

$$F_1(\mathbf{p}) = \mathbf{p}_1, \;\; F_2(\mathbf{p}_1) = \mathbf{p}_2, \;\; F_3(\mathbf{p}_2) = \mathbf{p}_3, \;\; \ldots\ldots .$$

To construct the sequence, this algorithm performs successive convolutions with a filter obtained from an auxiliary function named scaling function. We use a scaling function which has a $\mathbf{B}_3$ cubic spline profile. The use of a $\mathbf{B}_3$ cubic spline leads to a convolution with a mask of 5x5, all elements being scaled up to 256:

$$\begin{pmatrix} 1 & 4 & 6 & 4 & 1 \\ 4 & 16 & 24 & 16 & 4 \\ 6 & 24 & 36 & 24 & 6 \\ 4 & 16 & 24 & 16 & 4 \\ 1 & 4 & 6 & 4 & 1 \end{pmatrix}$$

As stated above, the wavelet planes are computed as the differences between two consecutive ap
$\mathbf{p}_{l-1}$ and $\mathbf{p}_l$. Letting $\mathbf{w}_l = \mathbf{p}_{l-1} - \mathbf{p}_l \;\; (l = 1, \cdots, n)$, in which $\mathbf{p}_0 = \mathbf{p}$, we can write the reconstructio

$$\mathbf{p} = \sum_{l=1}^{n} \mathbf{w}_l + \mathbf{p}_r \;\; .$$

In this representation, the images $\mathbf{p}_l \;\; (l = 0, \cdots, n)$ are versions of the original ir
(decreasing resolution levels), $\mathbf{w}_l \;\; (l = 1, \cdots, n)$ are the multiresolution wavelet planes
our case, we are using a diadic decomposition scheme. Thus, the original image $\mathbf{p}_0$
the image $\mathbf{p}_1$ double resolution than $\mathbf{p}_2$ and so on. If the resolution of image $\mathbf{p}_0$ is
of $\mathbf{p}_1$ would be $20m$, the resolution of $\mathbf{p}_2$ would be $40m$ etc.

4. WAVELET IMAGE FUSION M

The wavelet merger method is based on the fact that, in the wavelet dec
the successive versions of the original image at increasing scales. Thus
panchromatic image have spatial information that is not present
image merging can be carried out in two ways, as follows.

4.1. Substitution Method

In the wavelet substitution method, some of the wavelet planes of the multispectral image are substituted by the planes corresponding to the panchromatic image as follows:

1) Register the low-resolution multispectral image to the same size as the high-resolution panchromatic image in order to be superimposed.

2) Perform, as in section 2, histogram matching between the panchromatic image and the intensity component of the color image. Let **PAN** be the panchromatic image and **R**, **G** and **B** be the three bands of the multispectral image.

3) Decompose the R, G and B bands of the multispectral image to n wavelet planes (resolution levels). Usually $n = 3$ *or* 4.

$$\mathbf{R} = \sum_{l=1}^{n} \mathbf{w}_{\mathbf{R}l} + \mathbf{R}_r \qquad \mathbf{G} = \sum_{l=1}^{n} \mathbf{w}_{\mathbf{G}l} + \mathbf{G}_r \qquad \mathbf{B} = \sum_{l=1}^{n} \mathbf{w}_{\mathbf{B}l} + \mathbf{B}_r$$

4) Decompose the panchromatic high-resolution image accordingly

$$\mathbf{PAN} = \sum_{l=1}^{n} \mathbf{w}_{\mathbf{P}l} + \mathbf{PAN}_r$$

5) Replace the first wavelet planes of the R, G and B decompositions by the equivalent planes of the panchromatic decomposition

6) Perform the inverse wavelet transform

$$\mathbf{R}_{new} = \sum_{l=1}^{n} \mathbf{w}_{\mathbf{P}l} + \mathbf{R}_r \qquad \mathbf{G}_{new} = \sum_{l=1}^{n} \mathbf{w}_{\mathbf{P}l} + \mathbf{G}_r \qquad \mathbf{B}_{new} = \sum_{l=1}^{n} \mathbf{w}_{\mathbf{P}l} + \mathbf{B}_r$$

4.2. Additive Method

Another possibility is to add the wavelet planes of the high-resolution image directly to the multispectral image. The steps of this "additive" method are the following:

4.2.1. Adding to the RGB components

The first possibility[8] is to add the high-resolution information directly to the R, G and B bands. The steps of the method are:

1) Register the low-resolution multispectral image and perform histogram matching between the panchromatic image and the intensity component of the color image as before. Let **PAN** be the panchromatic image and **R** ,**G** and **B** be the three bands of the multispectral image.

2) Decompose only the panchromatic high-resolution image to n wavelet planes (resolution levels). Usually $n = 3$ *or* 4.

$$\mathbf{PAN} = \sum_{l=1}^{n} \mathbf{w}_{\mathbf{P}l} + \mathbf{PAN}_r$$

3) Add the wavelet planes of the panchromatic decomposition to the R, G and B bands of the multispectral image.

$$\mathbf{R}_{new} = \sum_{l=1}^{n} \mathbf{w}_{\mathbf{P}l} + \mathbf{R} \qquad \mathbf{G}_{new} = \sum_{l=1}^{n} \mathbf{w}_{\mathbf{P}l} + \mathbf{G} \qquad \mathbf{B}_{new} = \sum_{l=1}^{n} \mathbf{w}_{\mathbf{P}l} + \mathbf{B}$$

4.2.2. Adding to the L component

Another possibility, which we consider the best approach, is to incorporate the high-resolution information directly to the intensity component of the multispectral image. As explained in section 2 we use $L = \frac{R+G+B}{3}$ to represent the intensity component. We call this method Additive Wavelet on L (AWL) method for image merging. We[23,24] carried out a preliminary study of this approach. The steps of the method are the following:

Steps 1) and 2) as before. Thus,

$$\mathbf{PAN} = \sum_{l=1}^{n} \mathbf{w_{P}}_l + \mathbf{PAN}_r$$

3) Transform the RGB components of the multispectral image to the LHS representation. Let **L**, **H** and **S**, be the three componets of the multispectral image.

4) Add the wavelet planes of the panchromatic decomposition to the **L** component as follows:

$$\mathbf{L_{new}} = \sum_{l=1}^{n} \mathbf{w_{P}}_l + \mathbf{L}$$

5) Transform back the new LHS values into RGB representation.

In the substitution method, the wavelet planes corresponding to the multispectral image are discarded and substituted by the corresponding planes of the panchromatic image. However, in the additive method all the spatial information in the multispectral image is preserved. Thus, the main advantage of the additive method is that the detail information from both sensors is used. In practice, the results of the substitution method are similar to the results of the additive method but sligthly "defocused" showing that spatial information present only in the multispectral image is lost during the substitution process. Also, the results of the substitution method show some mixed colours in the boundaries of monochromatic areas. Thus, we will prefer always the additive method over the substitution method for the fusion of images.

The main difference between adding the panchromatic wavelet planes to the R, G and B bands as opposed to the L component is that, in the first case, panchromatic information is added in the same amount to all three bands, biasing the color of the pixel towards the gray, while in the second case the high-resolution information modifies only the intensity (L), preserving multispectral information in a better way. Thus, from the theoretical point of view, adding to the L component is a better choice than adding to the R, G and B bands. As stated in section 2, the reason for using the L component to represent the intensity instead of using I or L′ is that I ignores two of the RGB values and, using L′, the increments of intensity (obtained by adding the wavelet planes) are distributed, in some cases, not proportionally to the RGB values.

The advantages of using the wavelet image merging technique over the standard IHS or LHS methods are:

1) The spectral quality of the color image is preserved to a high degree.

2) The resolution of the panchromatic image is added to the solution without discarding the resolution of the multispectral image. Thus, the detail information from both images is used.

3) The total energy content (mean value) of a wavelet plane is 0. Thus, the total energy of the multispectral image is preserved.

4) The Additive Wavelet on L method (AWL) can be considered as an improvement on the classical IHS/LHS method in the sense that the intensity component is not substituted by the panchromatic image, but the highest resolution features not present in the multispectral image are introduced into the merged image by adding the first wavelet planes of the panchromatic image to the intensity component.

With regard to the number (n) of wavelet planes to add (or substitute in the substitution method), it depends on the ratio between the resolutions of the panchromatic and multispectral images. For example, if the panchromatic image is a $10m$ SPOT image and the multispectral is a $30m$ LANDSAT image, the first wavelet plane of the panchromatic image (w_1) contains the detail information between $10m$ and $20m$ while the second wavelet plane (w_2) contains spatial information between $20m$ and $40m$ that is over the size of the pixel of the LANDSAT image. Thus, in this case $n = 2$ would suffice. However, in practice the SPOT and LANDSAT images are taken at different epochs and to incorporate all the spatial information of the SPOT image is advised to use another wavelet plane ($n = 3$).

5. RESULTS

We applied the above methodology to merge SPOT and a LANDSAT (TM) images. The original panchromatic SPOT images have 10-m pixels while the original multispectral LANDSAT (TM) images have 30-m pixels. The LANDSAT original bands were converted to the (R, G,B) system using the following transformation: $R = \frac{B_5+B_7}{2}, G = \frac{B_3+B_4}{2}, B = \frac{B_1+B_2}{2}$. We present two examples in the following subsections. The first example is a low resolution image generated to have an original image to which compare the results. The aim of this first example is to quantify the gain of the different merging methods. The second example shows the application of our preferred method to a full resolution image.

5.1. Application to an inferior level

Because we do not have any LANDSAT (multispectral) image at 10-m resolution to compare with, the evaluation of the improvement of the additive wavelet method with respect to other merging methods is not easy. To solve this problem, in the first example, we applied the merging method to an inferior level of resolution, that is to say, on a SPOT panchromatic image at 30-m resolution and a LANDSAT multispectral image at 90m resolution. The result of the image fusion method is a merged multispectral image at 30m resolution which can be compared with the original LANDSAT image at 30m. In this first example we use a scene that includes both urban area and agricultural lots. The SPOT and LANDSAT images were taken at different epochs. This is an aditional problem for the merging process but we chose this example because it is the usual case when the images to merge come from different satellites. We do not show the images of this lower resolution example to save space for the second example which is at full resolution.

The available SPOT and LANDSAT (TM) original images were degraded to 30m and 90m resolution respectively. These degraded images are the images to merge. The images were registered and the SPOT image was photometrically corrected to present a histogram similar to the intensity component of the LANDSAT (TM) image. In order to compare the results, in this example we used the three definitions (I, L, L') for the intensity component. Then, we applied the additive wavelet-based image fusion methods explained above (AWRGB, AWI, AWL, AWL') and compared the results between them and to those given by the standard methods. In this example three wavelet planes were added.

To quantify the behavior of the standard and wavelet-based image fusion methods we computed the correlation between the different solutions and the original LANDSAT at 30m resolution image. To compute the correlation coefficient we use the standard coefficient:

$$Corr\ (A/B) = \frac{\sum_{j=1}^{npix} (A_j - \overline{A})(B_j - \overline{B})}{\sqrt{\sum_{j=1}^{npix} (A_j - \overline{A}) \sum_{j=1}^{npix} (B_j - \overline{B})}}$$

where $\overline{A}$ and $\overline{B}$ state for the mean value of the corresponding data set.

Table 1 shows the correlations between the different solutions and the original LANDSAT (TM) at 30m resolution image. As stated above, the different solutions are:

IHS	Standard substitution technique using I to represent the Intensity
L'HS	Ditto but using L'
LHS	Ditto but using L
AWRGB	Additive wavelets solution adding the high-resolution information to the R, G and B bands
AWI	Additive wavelets solution adding the high-resolution information to the I component
AWL'	Ditto but adding to L' component
AWL	Ditto but adding to L component

Table 1. Correlation between the standard methods (IHS, L'HS, LHS) and Additive wavelet-based methods (AWRGB, AWI, AWL', AWL) and the original LANDSAT Tematic Mapper image at 30-m resolution ($TM_{orig.}$).

	Correlation		
Images	Red	Green	Blue
$IHS/TM_{orig.}$	0.419787	0.307087	0.357959
$L'HS/TM_{orig.}$	0.589339	0.375114	0.376499
$LHS/TM_{orig.}$	0.668426	0.376118	0.420549
$AWRGB/TM_{orig.}$	0.861387	0.719150	0.756911
$AWI/TM_{orig.}$	0.804653	0.639473	0.711356
$AWL'/TM_{orig.}$	0.835543	0.694846	0.758833
$AWL/TM_{orig.}$	0.849157	0.721409	0.780618

The first, second and third lines of Table 1 show the correlation between the R, G, B bands of the standard solutions (IHS, L'HS, LHS) and the same bands of the original LANDSAT (TM) at 30-m resolution. Note that the best solution between the standard methods corresponds to the LHS method as expected from the theory exposed in section 2.

The last four lines of Table 1 show the correlation between the R, G, B bands of the additive wavelet-based solutions (AWRGB, AWI, AWL', AWL) and the same bands of the original LANDSAT (TM) at 30-m resolution. Note that the correlations of all the additive wavelet-based solutions are clearly higher than the correlations of the standard solutions. This means that the additive wavelet solutions preserve the spectral characteristics of the multispectral image to a greater extent than the standard IHS, L'HS and LHS solutions.

Looking to the correlations of the additive wavelet solutions, we can see that the correlations obtained for the AWL solution are higher than the AWI and AWL' methods. This is again in accordance with the theory that the L component represents the intensity component better that I or L' (section 2). The correlations of the AWRGB solution are very close to the correlations of the AWL method. Note that the correlation in the R band is even higher in AWRGB than in AWL, although this is compensated by the higher value of the correlation of the AWL in B band. However, as stated above, from the theoretical point of view, adding to the L component (AWL) is a better choice than adding to the R, G and B bands (AWRGB) because the last introduces a bias in the color of the pixel towards the gray.

Regarding to the degree of correlation obtained, although the target would be a correlation of 1.0 (perfect reconstruction of the original image), given that the LANDSAT and SPOT images were taken at different epochs this is not possible. Correlations of about 0.85 as the ones obtained with the additive wavelet method should be considered as the maximum correlation possible in this case.

Thus, the main conclusion of this section is that the additive wavelet solution on L (AWL) behaves better than the standard methods and the other additive wavelet-based methods in preserving both spatial and spectral characteristics of the original image during the image merging process. This is our preferred method which will be used to merge the images at full resolution of the following example.

5.2. Application to full resolution

In the second example we merge two SPOT and LANDSAT images at their full resolution. As stated above, the original SPOT image has 10-m pixels while the LANDSAT image has 30-m pixels. The images show a small portion of the Argentinian coast that includes urban area, agricultural lots and rivers. The images were registered and the SPOT image was photometrically corrected to present a histogram similar to the L component of the LANDSAT image. Then, we applied the AWL image fusion technique and compared the results to those given by the standard methods.

By technical constraints, in this paper, we cannot reproduce colors. Thus, we present hereafter the three bands of the image separatelly with the red band at left, the green band at center and the blue at right. This field can be used to test the spectral characteristics of the methods.

Figure 1. Detail of the LANDSAT image in R (left), G (center) and B (right) bands

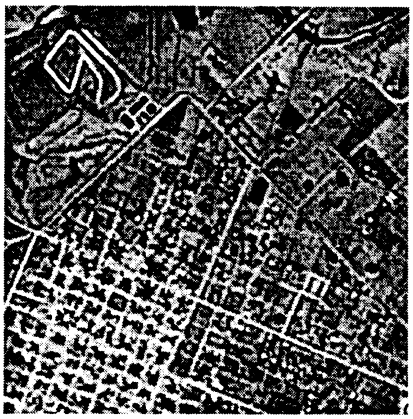

Figure 2. Detail of the SPOT image

Fig. 1 shows a detail of the original LANDSAT image in the three bands. Fig. 2 shows the same area of the SPOT image. The spatial resolution of the SPOT image is clearly better than the LANDSAT image as expected from the different pixel size of the detectors on both satellites. It is easy to see that the SPOT and LANDSAT images were taken at different epochs as it is usual when working with images from different satellites. Note, for example, the stretched white area at the right side of the LANDSAT image (Fig. 1), and other white spots which were not present when the SPOT image (Fig. 2) was taken. Also, there are several structures in the LANDSAT image that are clearly different from their appearance in the SPOT image.

Fig. 3 shows the result of the fusion of the LANDSAT and SPOT images by the standard LHS method. The increase in resolution with respect to the original LANDSAT image is evident. Most of the resolution of the SPOT image has been incorporated to the result. However, as stated above, the standard merging methods present spectral degradation and intensity dependence of the resulting color and a strong correlation between the merged image and the panchromatic intensity. Although this effect is stronger in the IHS solution (not shown) that in the LHS result of Fig. 3, this spectral degradationt can be seen qualitatively comparing the LHS result with the LANDSAT image (Fig. 1). Note that all three bands of the LHS solution resemble more to the SPOT image that to the corresponding band of the LANDSAT image. In particular, the white areas of the LANDSAT image are not present in the LHS result.

Fig. 4 shows the result of the fusion by the Additive Wavelet on L (AWL) method in the three bands. In this example three wavelet planes were added. As in the LHS solution, most of the resolution of the SPOT image was incorporated to the merged image. However, in this case, the spectral characteristics of the LANDSAT image are preserved better than in the standard mergers. Note the nearly identical tonalities of the three bands of the AWL result (Fig 4) and the corresponding bands of the original LANDSAT image (Fig. 1). In particular, the white areas of Fig. 1 are also present in Fig. 4 showing that the spectral characteristics of the LANDSAT image are well preserved

Figure 3. Detail of the fusion by the LHS method in R (left), G (center) and B (right) bands

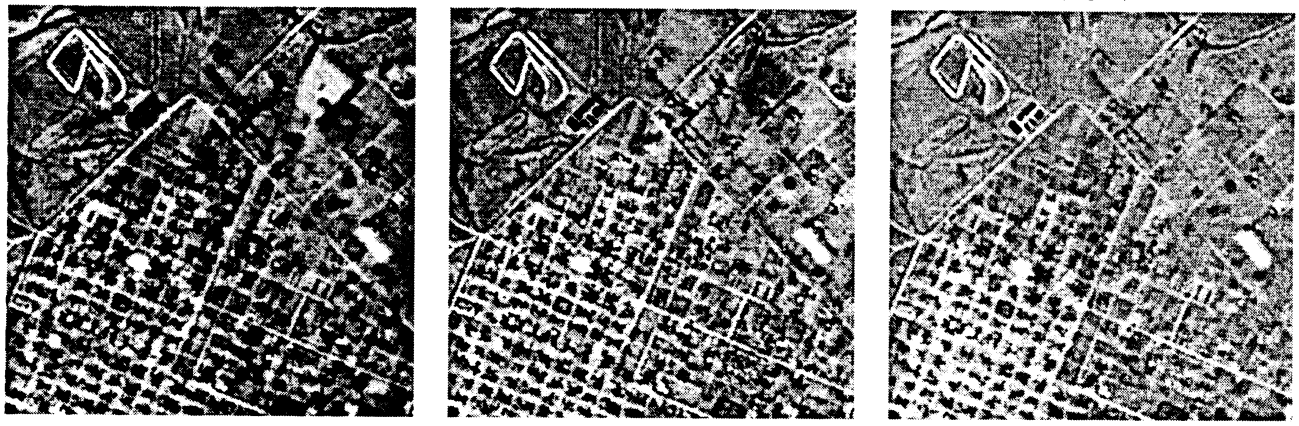

Figure 4. Detail of the fusion by additive wavelets on L method (AWL) in R (left), G (center) and B (right) bands

in the AWL solution.

In this example we do not have any original image (LANDSAT at 10-m pixels) to compare with. However, we can quantify the behavior of the AWL method in comparison with the standard methods by computing the correlation of the IHS, LHS and AWL solutions with regard to the SPOT and LANDSAT images. Note that in this case the target for the correlation is not 1.0. Also, a higher correlation with SPOT does not mean a better result.

Table 2 shows the correlations between the solutions by the IHS, LHS, and AWL merging methods and the original LANDSAT and SPOT images. The first line of Table 2 shows the correlation between the R, G, and B bands of the LANDSAT (TM) image and the SPOT image. The second and third lines show the correlation between the R, G, and B bands of the IHS and LHS solutions and the SPOT. The fourth line shows the correlations of the AWL solution. Note that the correlations of the IHS and LHS solutions are higher (especially in R) than the correlations of the AWL solution. This means that the standard solutions are closer to the SPOT image than the AWL solution. However, this is not a weakness of the AWL method. As stated above, there is strong correlation between the IHS and LHS merged images and the intensity of the panchromatic image. This "too high" correlation produces solutions that are closer to the SPOT image than desirable. The correlation is, however, lower in the additive wavelets solution. This is a positive fact because it means a lower dependence of the AWL solution on the Spot image.

Lines five to seven on Table 2 indicate the correlation between the same solutions and the LANDSAT (TM) image. Note that the correlation of our AWL solution is higher than of the IHS and LHS merging methods. This means that, as stated above in qualitative terms, the additive wavelet solution on L preserves the spectral characteristics of the multispectral image to a greater extent than the IHS and LHS solutions. Thus, the additive wavelet solution on L behaves better than the standard methods.

Table 2. Correlation between IHS, LHS and Additive Wavelets on L component (AWL) merging methods and SPOT and LANDSAT (TM) images.

	Correlation		
Images	Red	Green	Blue
TM/SPOT	0.190556	0.148597	0.31335
IHS/SPOT	0.910631	0.733614	0.830278
LHS/SPOT	0.758256	0.734147	0.774130
AWL/SPOT	0.486916	0.607829	0.723749
IHS/TM	0.417578	0.338116	0.120662
LHS/TM	0.722017	0.398778	0.117182
AWL/TM	0.922558	0.801127	0.740007

6. CONCLUSIONS

The additive wavelet-based methods are better suited for image merging than the standard techniques based on component substitution. These methods combine a high-resolution panchromatic image and a low-resolution multispectral image by adding some wavelet planes of the panchromatic image to the intensity component of the low-resolution image. Between the different wavelet-based methods studied, the additive wavelet method on the L component defined as $L = \frac{R+G+B}{3}$ (AWL) is which performs better. Using this method, the detail information from both images is preserved. The method is capable of enhancing the spatial quality of the multispectral image while preserving its spectral content to a grater extent. The AWL method does not modify the total energy of the multispectral image, since the mean value of each of the added wavelet planes is 0. The AWL method can be considered as an improvement on the classical IHS or LHS methods in the sense that the intensity is not substituted by the panchromatic image but the high-resolution of the panchromatic image is injected into the merged image by the addition of some wavelet planes of the panchromatic image to the intensity component of the multispectral low resolution image.

Acknowledgments

This work was supported in part by the DGICYT Ministerio de Educación y Ciencia (Spain) under grants no. BP95-1031-A and PB97-0903. Partial support was also obtained from the Institut Cartogràfic de Catalunya, the D.G.U. Generalitat de Catalunya and from the Gaspar de Portolà Catalan Studies Program of the University of California.

REFERENCES

1. T. Taxt and A.H. Schistad-Solberg, "Data fusion in remote sensing," in V. Di Gesu and L. Scarsi (eds.) Fifth workshop on Data Analysis in Astronomy, Erice, Italy Nov. 1996 (1996).
2. P.S. Chavez, S.C. Sides, and J.A. Anderson, "Comparison of Three Different Methods to Merge Multi-Resolution and Multispectral Data: Landsat TM and SPOT panchromatic," Photogrammetric Engineering and remote sensing **57,** n. 3, 295-303 (1991).
3. J. C. Tilton (Ed.), "Multisource data integration in remote sensing," NASA Conf. Publ. **3099** (1991).
4. J. W. Carper, T. M. Lillesand, and R. W. Kiefer, "The use of Intensity-hue-saturation transformations for merging SPOT panchromatic and multispectral image data," Photogrammetric Engineering and remote sensing **56,** 459-467 (1990).
5. V. K. Shettigara, "A Generalized component substitition technique for spatial enhacement of multispectral images using a higher resolution data set," Photogrammetric Engineering and remote sensing **58,** 561-567 (1992).
6. M. Datcu, D. Luca and K. Seidel, "Multiresolution analysis of SAR images," EUSAR'96, Konigswinter. Germany 375-378 (1996).
7. D. A. Yocky, "Image Merging and Data Fusion by Means of the Discrete Two-Dimensional Wavelet Transform," JOSA A **12,** n. 9, 1834-1841 (1995).

8. D. A. Yocky, "Multiresolution Wavelet Decomposition Image Merger of LANDSAT Thematic Mapper and SPOT Panchromatic Data," Photogrammetric Engineering and remote sensing," **62,** n. 9, 1067-1074 (1996).
9. B. Garguet-Duport, J. Girel, J. M. Chassery and G. Pautou, "The Use of Multiresolution Analysis and Wavelets Transform for Merging SPOT Panchromatic and Multispectral Image Data," Photogrammetric Engineering and remote sensing **62,** n. 9, 1057-1066 (1996).
10. T. Ranchin, L. Wald, and M. Mangolini, "The ARSIS method: A general solution for improving spatial resolution of images by the means of sensor fusion," In T. Ranchin and L. Wald eds., Proceedings of the International Conference: Fusion of Earth Data, Cannes, France, 53-58 (1996).
11. J. Núñez , X. Otazu, O. Fors and A. Prades, "Simultaneous image fusion and reconstruction using wavelets. Applications to SPOT + LANDSAT images," Vistas in Astronomy, in press (1998).
12. A. R. Smith, "Color gamut transform pairs," Comput. Graphics **12,** 12-19 (1978).
13. Association for Computing Machinery (ACM),"Status report of the graphics Standard Planning Committee," Computer Graphics **13,** n. 3, (1979).
14. Y. Meyer, "Wavelets. Algorithms and Applications," SIAM Press, Philadelphia, (1993).
15. R.K. Young, "Wavelet theory and its applications," Kluwer Ac. Pub., Boston, (1993).
16. I. Daubechies, "Ten Lectures on Wavelets," SIAM Press, Philadelphia, (1992).
17. C.K. Chui, "An Introduction to wavelets," Boston Ac. Press., Boston, (1992).
18. G. Kaiser, "A friendly guide to wavelets," Birkhauser, Boston, Englewood, NJ, (1994).
19. M. Vetterli and J. Kovacevic, "Wavelets and subband coding," Prentice Hall, (1995).
20. J. L. Starck and E. Pantin, "Multiscale Maximum Entropy Image Restoration,"' Vistas in Astronomy **40,** 563-569 (1996).
21. F. Rué and A. Bijaoui, "A multiscale vision model applied to astronomical images," Vistas in Astronomy **40,** 495-502 (1996).
22. J. L. Starck and F. Murtagh, "Image restoration with noise suppression using the wavelet transform," Astronomy and Astrophysics **288,** 342-350 (1994).
23. J. Núñez, X. Otazu, O. Fors and A. Prades, "Fusion and reconstruction of LANDSAT and SPOT images using wavelets," in T. Ranchin and L. Wald (eds.) Fusion of Earth Data. Sophia Antipolis (France) January 1998, 103-108 (1998).
24. J. Núñez, X. Otazu, O. Fors, A. Prades, V. Palá and R. Arbiol, "Image fusion using additive multiresolution wavelet decomposition. Applications to SPOT + LANDSAT images," to be published in JOSA A (1998).